THE JOURNAL OF BIOLOGICAL CHEMISTRY VOL. 285, NO. 52, pp. 41010–41018, December 24, 2010

Preventing Broken *Borrelia* Telomeres

ResT COUPLES DUAL HAIRPIN TELOMERE FORMATION WITH PRODUCT RELEASE[*][S]

Received for publication, May 31, 2010, and in revised form, October 3, 2010 Published, JBC Papers in Press, October 14, 2010, DOI 10.1074/jbc.M110.150060

Julien Briffotaux and Kerri Kobryn[1]

From the Department of Microbiology and Immunology, College of Medicine, University of Saskatchewan, Saskatoon, Saskatchewan S7N 5E5, Canada

Spirochetes of the genus *Borrelia* include the tick-transmitted causative agents of Lyme disease and relapsing fever. They possess unusual genomes composed mainly of linear replicons terminated by closed DNA hairpins. Hairpin telomeres are formed from inverted repeat replicated telomere junctions (rTels) by the telomere resolvase ResT. ResT uses a reaction mechanism similar to that of the type IB topoisomerases and tyrosine recombinases. ResT can catalyze three distinct reactions: telomere resolution, telomere fusion, and Holliday junction (HJ) formation. HJ formation is known to occur only in the context of a synapsed pair of rTels. To test whether telomere resolution was synapsis-dependent, we performed experiments with rTel substrates immobilized on streptavidin-coated beads. We report that telomere resolution by ResT is synapsis-independent, indicating that alternative complexes are formed for telomere resolution and HJ formation. We also present evidence that dual hairpin telomere formation precedes product release. This mechanism of telomere resolution prevents the appearance of broken telomeres. We compare and contrast this mechanism with that proposed for TelK, the telomere resolvase of ϕKO2.

Spirochetes of the genus *Borrelia* include important tick transmitted zoonotic pathogens that cause Lyme disease and relapsing fever maladies (1–5). *Borrelia* species possess unusual, highly segmented genomes with the majority of the replicons, including the chromosome, as linear dsDNAs terminated by covalently closed DNA hairpins referred to as hairpin telomeres (6–9).

The "end-replication problem" for linear DNAs is solved by the simplest of possible means; the hairpin telomeres eliminate the discontinuity in the DNA chain that causes the problem. Bidirectional replication from an internal origin produces, after replication through the hairpin telomeres, replication intermediates with replicated telomere (rTel)[2] junctions with inverted repeat sequence symmetry (10, 11, 44). Mother and daughter DNA molecules are covalently linked via the rTel junctions, which must be resolved by a specialized DNA breakage and reunion reaction, referred to as telomere resolution, that reforms the hairpin telomeres to allow for subsequent segregation. The essential, specialized telomere resolvase for *Borrelia* is known as ResT (13–15). A similar replication strategy has been demonstrated for the linear lysogen of the N15 bacteriophage, the best studied example of bacteriophages that possess linear prophage genomes terminated by hp telomeres (16–18).

ResT and other confirmed telomere resolvases have a catalytic domain that shares the protein fold and most of the catalytic side chains of the catalytic domain of tyrosine recombinases (19–22). Biochemical analyses have confirmed that telomere resolvases and tyrosine recombinases share a common chemical mechanism (13, 23). Additionally, ResT appears to have a hairpin-binding module similar to that found in cut-and-paste transposases; this module is implicated in DNA hairpin formation in both types of enzymes (24, 25).

The reaction of all characterized tyrosine recombinases proceeds via synapsis of the two recombining sites mediated by an enzyme tetramer; cleavage and strand exchange of the equivalent strand in each duplex forms a Holliday junction (HJ). The HJ then undergoes a modest isomerization leading to cleavage and strand exchange of the remaining pair of DNA strands to produce the recombinant products (26). By contrast, the co-crystal structure of a bacteriophage telomere resolvase (TelK) that captures TelK with its substrate after cleavage but before hairpin formation shows a dimer acting on a single reaction site (20).

ResT can catalyze three distinct reactions: telomere resolution (formation), telomere fusion, and HJ formation (13, 27, 28). In principle, telomere resolution and fusion could be catalyzed by a dimer of ResT as is telomere resolution catalyzed by TelK. However, the HJ formation reaction catalyzed by ResT occurs in the context of a synapsed pair of rTels as it always does in the reactions of tyrsosine recombinases (28, 29). Therefore, it has been unclear whether ResT could form alternative dimeric, unsynapsed, and synapsed tetrameric complexes to catalyze the telomere resolution and HJ formation reactions, respectively, or whether both reactions occur in a complex with two synapsed rTels and a tetramer of ResT. The possible alternative reaction schemes for telomere resolution if the reaction is synapsis-dependent *versus* -independent is summarized below (Fig. 1).

* This work was supported by Canadian Institutes for Health Research Grant MOP 79344.

[S] The on-line version of this article (available at http://www.jbc.org) contains supplemental Table 1 and Figs. 1–3.

[1] To whom correspondence should be addressed: Dept. of Microbiology and Immunology, College of Medicine, University of Saskatchewan, Saskatoon, Saskatchewan S7N 5E5, Canada. Tel.: 1-306-966-8818; Fax: 1-306-966-4298; E-mail: kerri.kobryn@usask.ca.

[2] The abbreviations used are: rTel, replicated telomere; hp, hairpin; HJ, Holliday junction; CP, cleavage product; DSP, dithiobis(succinimidyl propionate); ResT, telomere resolvase; TelK, telomere resolvase.

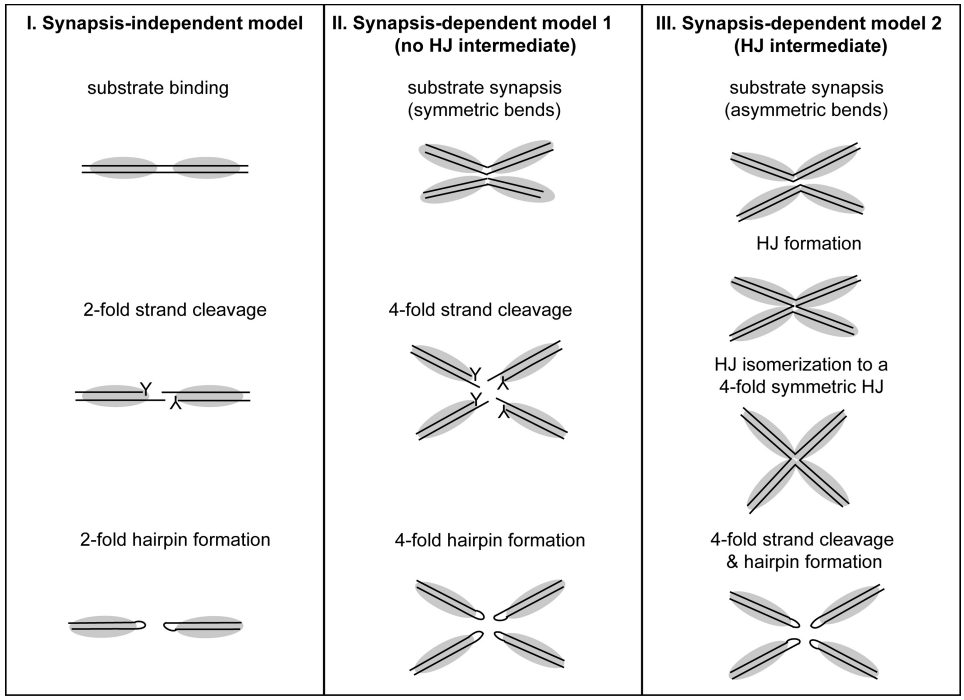

FIGURE 1. **Models of synapsis-independent and synapsis-dependent telomere resolution.** Model I (*I*) features a dimer of ResT acting on a single rTel. Both strands are cleaved simultaneously. This establishes a transient intermediate in which a monomer of ResT is covalently attached to each DNA strand via 3′-phosphotyrosyl linkages (represented by the *Y* in the schematic) that store the bond energy of the substrate. The 6-nt 5′-OH terminated overhanging strands attack the phosphotyrosyl bonds on the opposing strands to form two hairpin telomeres. This is the mode of action of the bacteriophage telomere resolvase, TelK. Model II (*II*) features a tetramer of ResT acting on two rTels in a synaptic complex. It is in the context of this synapse that the 4-fold DNA cleavage and hairpin formation reactions occur. In this model, synapsis is only required to activate reaction chemistry that proceeds as in Model I. This mode of regulation of enzyme activity is a feature of the reactions of many restriction enzymes and of the transposon excision reaction catalyzed by cut-and-paste transposases (*e.g.* Refs. 42, 43). Model III (*III*) also features a tetramer of ResT acting on two rTels in a synaptic complex. This model posits transition through a HJ intermediate. The HJ is isomerized to a 4-fold symmetric structure, and the 4-fold strand cleavage and hairpin formation reactions occur as in Model II. The HJ intermediate is a feature of the reactions of the tyrosine recombinase family of enzymes, with which ResT shares a catalytic domain (see Introduction). The prototypical tyrosine recombinase, λ integrase, has been reported to produce DNA hairpins (and three-way junctions) from reaction with certain modified HJs (12, 37).

EXPERIMENTAL PROCEDURES

Oligonucleotides, Beads, and Proteins—All oligonucleotides were purchased from Integrated DNA Technologies. The streptavidin coated beads were 1 μm paramagnetic Dynabeads® MyOne™ streptavidin C1 from Invitrogen. All reactions used N-terminal (His_6) tagged wild type ResT purified as reported in Ref. 25.

Immobilization of rTel Substrates—For each 0.6 pmol of 5′-^{32}P end-labeled, biotinylated DNA substrate, the substrate was mixed with 1.5 μl of 1 μm paramagnetic Dynabeads® MyOne™ streptavidin C1 (Invitrogen). The mixture was incubated in 50 μl of buffer containing 50 mM Tris-Cl, pH 7.4, 150 mM NaCl, 1.0 mM EDTA, 0.05% Tween 20. Incubation was at room temperature for 30 min with gentle agitation. The beads were then washed three times in 500 μl of the same buffer to remove unbound substrate.

Reactions with rTels Immobilized on Streptavidin Beads—0.6 pmol of the bead-immobilized rTel were then placed in 40 μl of buffer containing 50 mM Tris-Cl, (pH 8.5), 100 mM NaCl, 1.0 mM EDTA, 0.05% Tween 20, 1 μg/ml BSA, 10% glycerol, and 11 μg/ml of ResT. Incubation was at 30 °C for 45 min with gentle rotation. Bead and supernatant fractions were separated by application of the test tubes to a DynaMag-2™ magnetic test tube rack (room temperature for 20 s; Invitrogen). Biotinylated product (and substrate) bound to the beads were dissociated by heating the complex for 2 min at 95 °C in a buffer containing 10 mM EDTA, pH 8.2, and 95% (v/v) formamide. The free products in the supernatent were treated in the same manner prior to PAGE analysis. The reaction products were separated using a 10% polyacrylamide electrophoresis gel containing 7 M urea and 1× TBE buffer at 27 V/cm and then documented on a Storm 860 PhosphorImager.

DSP Cross-linking Assays—Reactions contained 25 mM Tris-Cl, pH 8.5, 150 mM NaCl, 1 mM EDTA, 0.03 pmol of radiolabeled DNA substrate, and 4 μg/ml ResT. 240 μl reactions were incubated at 30 °C for 45 min. Dithiobis(succinimidyl propionate) (DSP; Pierce) was added at 10 and 50 μg/ml (final concentration) in 40 μl of each aliquot for 15 min at room temperature. A stock solution of 25 mg/ml DSP in dimethyl sulfoxide was prepared immediately before use. Tris/Lysine was added to a final concentration of 30 mM for both components to quench excess unreacted DSP (room temperature for 5 min). The reaction products were resolved using a 20-cm 4.5% polyacrylamide electrophoresis gel containing SDS and 1× TAE buffer at 200V for 2 h and visualized after scanning the gels with a Storm 860 PhosphorImager.

RESULTS

A Physical Test for Synapsis (In)dependence of Telomere Resolution

Experimental Rationale—As a direct physical test of whether telomere resolution is synapsis-dependent or -inde-

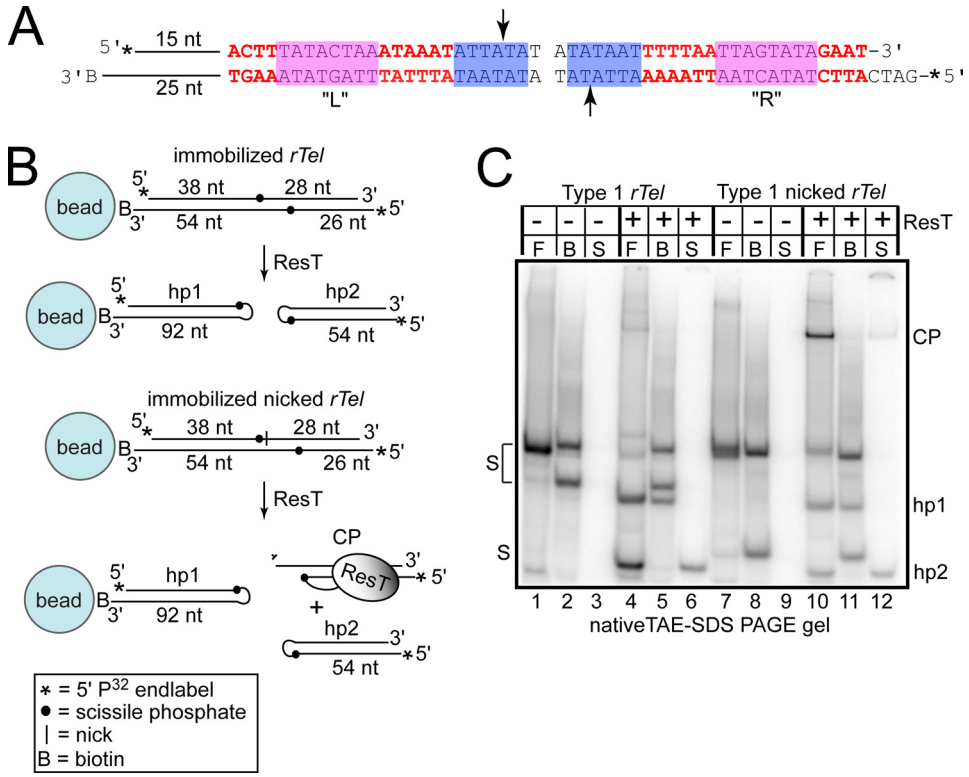

FIGURE 2. **Reactions with immobilized type 1 rTels.** *A*, the type 1 rTel used in this study. To aid the annealing of the oligonucleotides into an rTel, the normal dyad symmetry of native rTels was broken by having distinct sequences on the left (*L*) and right (*R*) sides in positions where the sequence of different type 1 rTels varies (*red letters*). The *magenta* and *blue boxes* highlight sequences found in all type 1 rTels; the *arrows* indicate the scissile phosphates. 15 bp of the nontelomeric sequence was added the *left side*, and the biotin moiety (*B*) is on the terminus of an additional 10 nt of ssDNA. These extensions were added to eliminate steric clash and to increase the gel mobility differences of the substrate and products. The *asterisks* on the 5′ ends represent ^{32}P end labels. The *L* sequence is derived from the sequence of the right telomere of lp17 and lp56. The R sequence is derived from the ChromR telomere (31). *B*, schematic of the substrate and experimental design. The substrate in *A* is immobilized on a 1-μm streptavidin-coated paramagnetic bead via a 3′-biotin modification present on the bottom strand of the substrate. The nucleotide distance between the termini and the scissile phosphates is indicated. The total chain length of the hairpin products (hp1 and hp2) is also shown. The bottom schematic pictures a nicked suicide rTel with a strand discontinuity 1 nt 3′ of the cleavage site on the top strand. Post-cleavage diffusion of this nucleotide prevents strand resealing to reconstitute substrate and slows the hairpin formation reaction of the product released into the supernatant allowing accumulation of CP, wherein ResT is covalently attached to the bottom strand. *C*, 10% native TAE-SDS-PAGE analysis of telomere resolution reactions with the substrates in *A* and *B*. In the reaction key *above the gels*, *F* is free substrate (no beads); *B* is the bead fraction after dissociation from the beads; and *S* is the supernatant. The supernatant and bead fractions are separated by application of the reaction to a magnetic test tube rack. On the gel labels, *S* is substrate. Unreacted substrate splits into two bands after the treatment used to dissociate immobilized substrate from the (95 °C for 2 min in formamide). hp1 & hp2 are the hairpin telomere products.

pendent, we adopted the approach of physically immobilizing the rTel substrate on a physical matrix (3′-biotin modified substrates and streptavidin-coated 1-μm paramagnetic beads; Fig. 2*B* and "Experimental Procedures"). The rationale for the experiment is that when the substrate is immobilized on beads at subsaturating conditions (2.2% of bead substrate binding capacity) synapsis with another rTel is prevented unless excess free substrate is added in solution to the reactions (30).

A Physical Test for Synapsis (In)dependence of Telomere Resolution

Substrate Design—Natural substrates are completely dyad symmetric. Such inverted repeat symmetry favors intramolecular annealing, yielding hairpins rather than rTels. It was therefore necessary to design substrates in which the inverted repeat is disrupted by constructing rTels that are hybrids of the sequence of distinct hairpin telomeres that possess comparable specific activities *in vitro* (see Figs. 2*A* and 3*A*) (31). Additionally, 15 bp of a nontelomeric sequence were added to the left side of the substrate. This substrate design allows efficient assembly of rTels from two oligonucleotides without contaminating hairpins and allows differentiation of products formed on the left and right sides of the rTel. The nontelomeric 15 bp also increase the distance between the substrate and the bead to reduce the effects of steric clash on the reaction. The rTel is tethered to streptavidin-coated paramagnetic beads via a 3′-biotin moiety synthesized into the oligonucleotide that comprises the bottom strand of the substrate. With this substrate design, resolution of the rTel when it is immobilized results in the larger hairpin telomere (hp1) remaining attached to the bead, whereas the smaller hairpin telomere (hp2) is released into the supernatant (Fig. 2*B*).

Because use of such artificial asymmetric rTel substrates has not been reported previously, we ran preliminary experiments to confirm that an asymmetric rTel and a nicked or "suicide" version of the asymmetric rTel yield the same products as their symmetric counterparts. The results of this analysis are shown in supplemental Fig. 1. The native 10% native TAE-SDS-PAGE gel analysis shows that the same pattern of products is produced from symmetric and asymmetric versions. The protease K digestion removes ResT covalently

attached to the cleavage product (CP) confirming our assignment of this product in the reactions with asymmetric rTels by analogy with previous characterization of reactions with symmetric rTels (supplemental Fig. 1*B*, native gel, *lanes 3*, *6*, *9*, and *12*). Also apparent from the native gel analysis is the problem of incomplete or improper annealing of a fraction of the symmetric substrates; this problem is especially prominent for the symmetric nicked rTel (supplemental Fig. 1*B*, native gel, *lanes 4* and *10*). The 10% denaturing TBE-urea PAGE analysis confirms the assignment of the hp1 and hp2 products as hairpin telomeres and that both asymmetric and symmetric versions of the substrates yield products of identical size (supplemental Fig. 1*B*, denaturing gel, *lanes 2*, *4*, *6*, and *8*).

Synapsis Independence of Telomere Resolution—Fig. 2*C* documents the results of reactions with an immobilized rTel. The first three lanes are controls without ResT. The *first lane* establishes the efficacy of substrate annealing. *Lane 2* shows the rTel after immobilization, mock incubation, bead collection by magnet, and dissociation of the rTel from the beads by incubation at 95 °C in formamide. This establishes the position on the gel of the bands that represent unreacted substrate after the procedure for bead dissociation. *Lane 3* is the supernatant of the mock reaction, and the emptiness of this lane shows that all the added substrate was absorbed to the beads. *Lane 4* shows the biotinylated rTel reacted with ResT in the absence of streptavidin-coated beads. This is referred to as a "free" reaction (indicated by *F* in the gel reaction key). The reaction with the immobilized substrate (*lanes 5* and *6*) shows that immobilization does not prevent reaction. The hp1 and hp2 products appear in the expected fractions. Examination of an aliquot from each reaction on a TBE/urea polyacrylamide gel confirmed that the products observed were indeed DNA hairpins (data not shown). The immobilization does not block a required synapsis step as titration of free rTel lacking the biotin modification further inhibits the reaction (data not shown). These results argue against the two synapsis-dependent models presented in Fig. 1.

It should be noted that although immobilization of the substrate did not block reaction, it did lower the level of reaction (Fig. 2*C*; *lanes 5/6 versus 4*). The 3′-biotin moiety, *per se*, has no effect on reaction efficiency as confirmed by comparison of control free reactions with biotin-containing substrates and the same substrates lacking the biotin modification (data not shown). The reduced reaction levels seen with the immobilized substrates is caused by a combination of the effects of bead addition independent of substrate immobilization and by a direct diminution of reaction kinetics caused by the immobilization (see supplemental Fig. 2). The immobilization-independent effect of bead addition reduces the amount of substrate converted into products but does not affect kinetics (supplemental Fig. 2, no biotin substrates, − *versus* + bead addition, *top gel*). Despite this minor effect on reaction efficiency, biotin-mediated immobilization of substrates provides a powerful tool to visualize telomere resolution products and to follow product release.

Assaying Effect of Immobilizing a Suicide Substrate—To assay the effect of substrate immobilization on DNA cleavage and hairpin telomere formation, we designed a substrate that allowed us to study these reaction steps separately with a single substrate (Fig. 2*B*, *lower panel*). The substrate is the same rTel used in Fig. 2*B* (*upper panel*) modified by introduction of a discontinuity in the top DNA strand one nt 3′ of the scissile phosphate. This is a so-called suicide substrate since cleavage of the top strand causes the one nt distal to the cleavage site to diffuse away, blocking strand resealing to reconstitute the substrate and to slow (but not completely block) hairpin formation on the right side of the substrate; ResT covalently attached to the cleaved substrate becomes trapped on the DNA and is readily identified on an SDS-containing polyacrylamide gel as a CP (Fig. 2, *lane 10*) (32).

Fig. 2*C* shows the result of immobilization of this substrate. Substrate assembly and absorption to the beads was assessed as before (Fig. 2*C*, *lanes 7–9*). Reaction with the immobilized nicked rTel yielded hp1 in the bead fraction and the covalent ResT-DNA CP and hp2 in the supernatant fraction (*lanes 11* and *12*, respectively). Examination of an aliquot from each reaction on a TBE/urea polyacrylamide gel confirmed that the products observed were DNA hairpins rather than protein-free double strand breaks (data not shown).

The free reaction of the nicked rTel yielded the expected preponderance of the CP *versus* hp2 indicating that the presence of the top strand nick inhibits hp2 formation (Fig. 2*C*, *lane 10*). However, immobilization of the nicked rTel resulted in a release into the supernatant of a much less CP relative to hp2 than expected (Fig. 2*C*) (12). This hinted at possible communication between the hairpin formation events prior to product release.

Assaying Immobilized Type 2 rTels—The telomeres of *Borrelia burgdorferi* vary in sequence with only one sequence motif, referred to as box 3, occurring in all telomeres at positions 14–21. The various telomere sequences divide into three types based on the presence/absence and relative spacing of another sequence motif referred to as box 1. (Box 1 and 3 motifs are represented as *blue* and *magenta shaded boxes* in Figs. 2 and 3.) Only type 1 and 2 rTels are efficiently resolved *in vitro* by ResT (15, 31). The rTel assayed in Fig. 2 represents a type 1 telomere. We therefore designed and tested the effect of substrate immobilization on a type 2 rTel as well (Fig. 3).

With the initial version of the type 2 substrate that we designed and tested, the asymmetrization of the sequence of the rTel needed for efficient substrate assembly led to very unequal yields of the two hairpins in free reactions with much more hp2 formed than hp1 (Fig. 3*B*, *lane 4*). This marked bias is not due to unequal labeling of the strands (Fig. 3*B*, denaturing gel, *lane 1*). Immobilization of this substrate equalized the yield of hp1 *versus* hp2. The bias in hairpin formation seen in the free reaction of rTel version 1 (LR) could be due to the presence of the extra nontelomeric sequence present on the left side of the substrate or to the sequence differences (7/25 bp) between the "L" and "R" sequences. To distinguish between these possibilities, we swapped the L and R sequences to produce rTel version 2 (RL; Fig. 3*A*). This RL arrangement eliminates the hp2 formation bias in free reactions seen with the LR substrate (Fig. 3*B*, *lane 10*). This indicates that the bias in hp formation was due to the telomeric sequences (or spe-

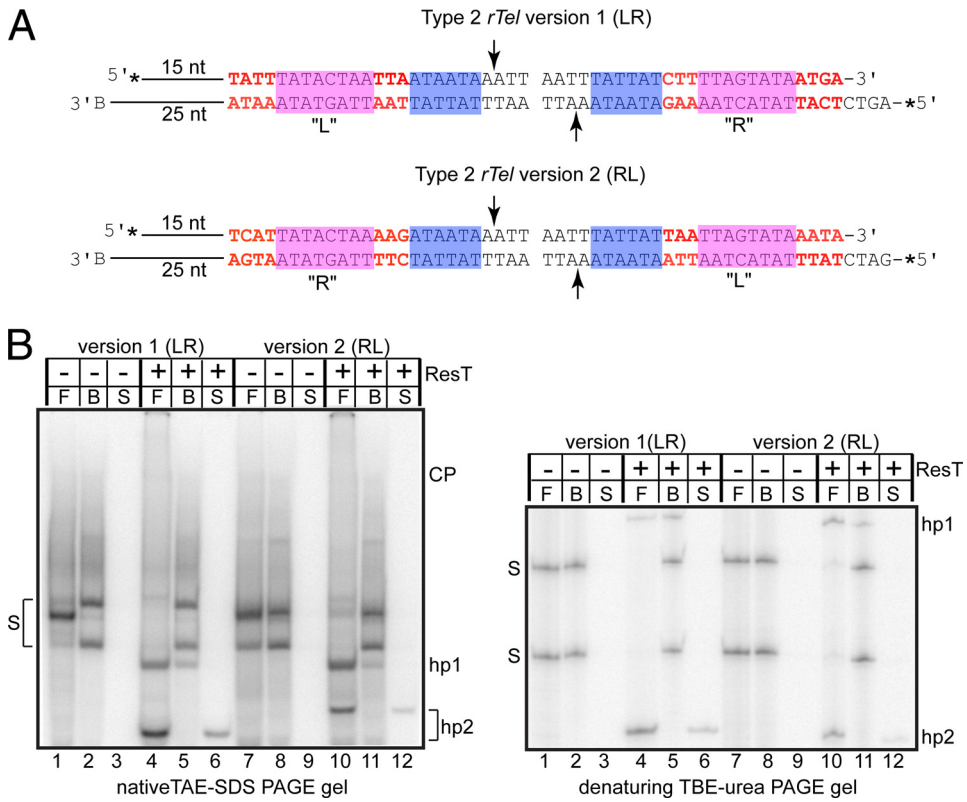

FIGURE 3. **Reactions with immobilized type 2 rTels.** *A*, a schematic of the substrates used. A comparison with Fig. 2*A* will reveal that type 2 rTels differ from type 1 rTels by the sequence of box 1 (shaded in *blue*) and by the relative spacing between of the box 1 and box 3 sequences (the latter shaded in *magenta*). Version 1 (LR) of a type 2 rTel that we tested displayed a large bias in the ability to form the hairpin telomeres on one side of the substrate relative to the other, so we constructed a second version where the L and R sequences were switched to yield Type 2 rTel version 2 (RL). As in Fig. 2, the sequences that differentiate the L and R sides are noted with *red characters*. The L sequence is derived from the left telomeres of lp28-2 and lp36. The R sequence is derived from the right telomere of lp28-4 (31). *B*, 10% native TAE-SDS-PAGE and 10% denaturing TBE-urea PAGE analysis of telomere resolution reactions with the substrates in *A*. The gel labels are as indicated in Fig. 2*C*.

cifically the L sequence juxtaposition with the nontelomeric sequences) rather than due solely to an effect of the nontelomeric sequences. Immobilization of rTel version 2 (RL) markedly reduced overall reaction yield; comparable relative levels of hp1 and hp2 were recovered in the bead and supernatant fractions (Fig. 3*B*, *lanes 11* and *12*).

Unexpectedly, the mobility in a native gel but not the nucleotide chain length of hp2 product differs between the LR and RL versions of the substrate (Fig. 3*B*, *lanes 4* and *6 versus lanes 10* and *12*, native *versus* denaturing gels). This indicates that hp2 produced from reaction with the RL substrate possesses more intrinsic curvature than hp2 produced from the LR substrate (*e.g.* Ref. 33). The mobility in native gels of the two substrates is equivalent, showing that the sequence swap has not affected the overall curvature of the substrates. This would seem to indicate that the telomeric R sequences or the non-telomeric sequence must cancel out the intrinsic curvature of the L sequence.

A key difference between free and immobilized reactions is that in the immobilized reactions only hairpin products that have been released are visualized; this is, by definition, the case for the products in the supernatant. The reaction products from free reactions represent both products that have been released as well as products that may be present in ResT-DNA complexes in which only one hairpin telomere has formed. This is the case because the results of the free reactions are visualized after termination of the reaction with SDS for application to the gels, whereas the results of the immobilized reactions are only visualized after the bead and supernatant fractions are separated by application of the reactions to a magnetic test tube rack to pull down the paramagnetic beads. Therefore, the equalization of hairpin telomere yield in immobilized reactions using a substrate with a large hairpin formation bias (version 1 (LR)) suggested that hairpin telomeres are not released until both hairpin telomeres form.

Hairpin Formation Occurs Prior to Product Release—To more rigorously test this contention, we performed time course experiments with a nicked rTel under conditions where we could manipulate the relative hairpin formation rates of the two hairpin telomeres and tested the effect of immobilization on the time course (Fig. 4). The nicked type 1 rTel used in Fig. 2 was employed again. As noted for that experiment, hp2 formation proceeds more slowly than hp1 formation as the 5′ overhang that results from cleavage is one nt too short, and consequently, the hairpin that forms must do so without a complementary base pair at the site of strand resealing (Fig. 2) (32). Therefore, one can infer that hairpin formation under standard conditions is homology-dependent. We have discovered that this homology dependence can be partially alleviated by supplementing the reaction buffer with glycerol to a final concentration of 10%. Addition of glycerol

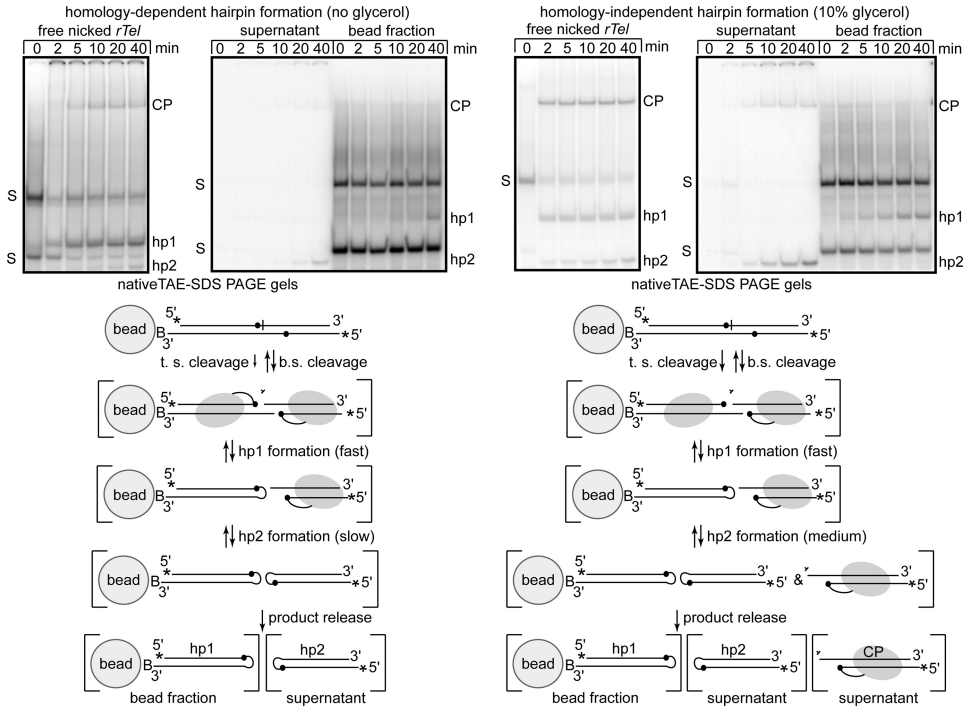

FIGURE 4. **The effect of immobilization on time course reactions with an rTel that forms the two hairpin telomeres at different rates.** 10% native TAE-SDS-PAGE analysis of telomere resolution time courses comparing free *versus* immobilized reactions under homology-dependent (very slow hp2 formation) and partially homology-independent (faster hp2 formation) conditions using the nicked type 1 rTel presented in Fig. 2. Under the gels, interpretations of the reaction occurring under the two regimes is presented. Both the strands of the substrate are cleaved; top strand (*t.s.*) cleavage is slower due to the presence of the nearby nick (32) and irreversible due to the diffusion away of the nucleotide distal to the scissile phosphate. Bottom strand (*b.s.*) cleavage is reversible as it occurs on the intact strand. Subsequent to cleavage the two hairpins are formed at different rates. The hairpins appear not to be released until both are formed substantially slowing the reaction relative to the free reaction in which all products whether released or not are visualized. The case of the time course performed under partially homology-independent conditions differs in two key respects: (i) hp2 formation is substantially accelerated, and this is mirrored by a corresponding increase in the rate of hp1 formation, and ii) CP is released into the supernatant indicating that successful hp2 formation and product release have been partially uncoupled.

reduces the disparity in the reaction rates of hp1 *versus* hp2 formation (Fig. 4*A*, free reaction panels).

Under homology-dependent conditions, hp1 formation in free reactions is essentially complete by 5 min; hp2 does not start to appear until the 10-min time point, and only a small amount has been produced by the 40-min end point. The cleaved but not yet hairpinned right side of the substrate is apparent on the gel as the CP band; top strand cleavage is somewhat slower than bottom strand cleavage, but the major effect for hp2 formation is on the rate of the hairpinning step (Fig. 4) and (32). Upon immobilization of this substrate under these conditions, the yield of the hairpins is equalized, and the reaction proceeds at the slow rate of hp2 formation (compare hp2 appearance in the supernatant *versus* hp1 appearance in the bead fraction; Fig. 4).

Supplementing the reaction buffer with glycerol increases the reaction rate of top strand cleavage and hp2 formation (Fig. 4*A*, *homology-independent free panel*). This increase in the reaction rate of hp2 formation was accompanied by a corresponding and equal increase in the rate of hp1 formation in reactions with immobilized nicked rTel (Fig. 4*A*, *homology-independent immobilized panel*). Essentially identical results were obtained with a nicked type 2 rTel (data not shown). An interpretive reaction scheme is presented under the gels for the two conditions (Fig. 4). The results in Fig. 4 strengthen the conclusion that hairpin formation precedes product release.

Protein-protein Cross-linking ResT in a ResT-DNA Complex That Has Formed Only One Hairpin—We reasoned that if the slow formation of hp2 in the nicked rTel substrate used in Fig. 4 prevented the dissolution of the ResT-DNA complex catalyzing telomere resolution and product release, then we should be able to visualize this complex by protein-protein cross-linking. The CP in Figs. 2 and 4 represents a monomer of ResT covalently linked to a radiolabeled half-site; addition of a protein crosslinker (DSP) should trap an additional monomer of ResT on this half-site if a dimeric ResT-DNA complex performing telomere resolution persists until hp2 formation is complete. Fig. 5 presents the results of DSP addition to a reaction under conditions that maximize the yield of CP but before significant amounts of hp2 has been formed (no glycerol supplement, 4 μg/ml ResT in a 30 °C, 30-min incubation). *Lane 2* shows the reaction with a nicked rTel without DSP addition; there is quantitative conversion of the substrate into hp1 and CP (the small amount of hp2 formed runs off the bottom of this gel). As expected, addition of DSP (*lanes 3* and *4*) trapped an additional monomer of ResT onto the radiolabeled half-site. ResT is prone to aggregation (34) and a significant proportion of the cross-linking has resulted in a shift into the well, especially at the higher concentration of DSP tested (*lane 4*; 50 μg/ml). Essentially identical results were obtained when the cross-linking experiment was repeated with an immobilized version of the nicked rTel (see supplemental Fig. 3).

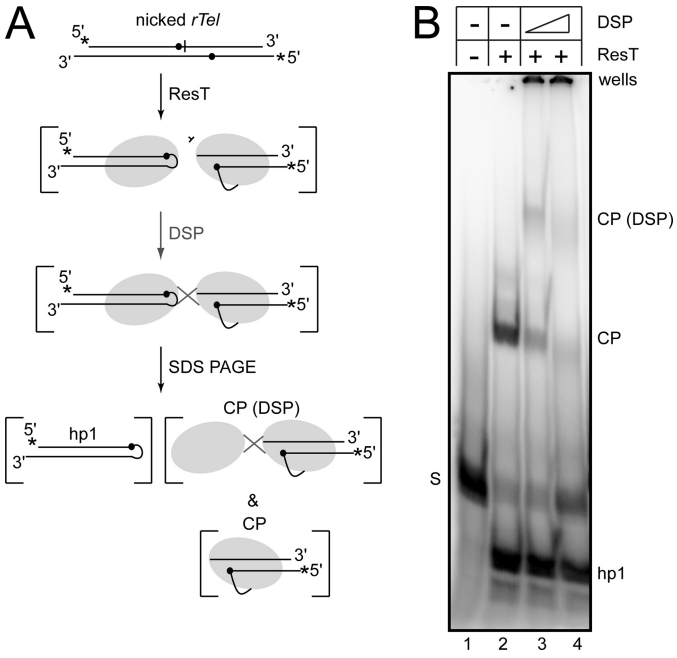

FIGURE 5. **DSP cross-linking a second ResT protomer to the ResT protomer trapped in CP produced by reaction with a nicked rTel.** *A*, schematic representation of the protein-protein cross-linking experiment with the type 1 nicked rTel used in Figs. 2 and 4 (see Fig. 2, *A* and *B*). ResT is incubated with the nicked rTel under conditions that maximize the yield of the CP in which ResT is covalently attached to the radiolabeled DNA (no glycerol in the reaction buffer; 30 °C for 30 min incubation). DSP was added to induce cross-linking. The resulting cross-linked species are visualized by 4.5% TAE-SDS-PAGE. ResT is represented by *shaded ovals*, the *line* connecting the ResT to the scissile phosphate (●) indicates the covalent 3′-phosphotyrosine linkage trapped by cleavage next to the nick on the top strand. CP and CP (DSP) are covalent ResT-DNA complexes with the radiolabeled half-site derived from the right side of the rTel after cleavage; cross-linking is visualized by virtue of attachment to this half-site. hp1 is the hairpin telomere derived from the left side of the rTel. *B*, 4.5% TAE-SDS-PAGE analysis of the results of DSP cross-linking a reaction with a type 1 nicked rTel. The *key above the gel* indicates whether ResT has been added to the incubation and if DSP treatment has followed the reaction (two concentrations of DSP were used; 10 and 50 μg/ml). The gel labels are explained in *A*. A 20-cm long vertical gel apparatus was used.

DISCUSSION

Mechanism of Hairpin Telomere Formation—Different mechanisms of hairpin telomere formation seem to be operative for the two best characterized telomere resolvases: ResT and TelK (also referred to as a protelomerase). The leading models for each are presented in Fig. 6. In both models, the 6 bp between the scissile phosphates must be deformed as a prelude to the breaking of these bp and the formation of the hairpin telomeres. The hairpin telomeres are a higher energy structure than the original duplex because only one base pair, at most, from between the cleavage sites would reform at the base of each hairpin loop (20, 35). Therefore, both models must explain where the energy for their formation is derived.

For ResT, the hairpin-binding module is thought to play a crucial precleavage role by predisposing the DNA between the cleavage sites to assume a conformation prepositioned to cause hairpin formation once the substrate DNA has been cleaved (25). The hairpin-binding module was identified by sequence homology to a region of Tn5 transposase crucial for hairpin formation in the transposon excision reaction of Tn5 (24, 36). Mutation of this module in ResT results in a cleavage defective telomere resolvase. This defect can be rescued by introduction of the heteroduplex at the central 2 bp of the rTel, which predisposes the DNA to spontaneously fold back into DNA hairpins (25). The hairpin-binding module may actively distort the DNA or stabilize something akin to a preformed bulged DNA structure. This role is structure-specific rather than sequence-specific, as ResT recognizes and resolves 19 different telomeric sequences that include six distinct sequences between the scissile phosphates (31). The hairpin-binding module is not well conserved in TelK (20).

Experimental data indicate that the energy stored in the substrate in the form of DNA supercoiling plays an important role in telomere resolution by being used to aid assembly of a chemically competent "cross-axis" complex, a process that is probably equivalent to dimerization of ResT on its substrate (see Fig. 5). This does not occur easily on linear or relaxed DNA (25, 32, 34). Once this has occurred, DNA cleavage and hairpin formation rapidly follows, all within the context of the cross-axis complex (this study). DNA supercoiling has not been reported to affect the reaction of the bacteriophage telomere resolvases typified by TelN and TelK (16, 23). The model of hairpin telomere formation for TelK differs from that for ResT mainly by hairpin telomere formation proceeding by use of the energy of a strained dimer complex being used for its dissolution concomitant with or preceding formation of the hairpin telomeres (20).

A domain of TelK critical for hairpin telomere formation has also been discovered and is referred to as the stirrup domain. The stirrup domain interacts with distal sites in the substrate; this interaction stabilizes a large (73°) bend induced by TelK binding. The stirrup domain plays a post-cleavage role in hairpin formation; its deletion does not affect the ability of TelK to cleave its substrate but blocks formation of the hairpin telomeres. The energy of the DNA bend that the stirrup domain stores in the complex is thought to aid the dissolution of the complex once DNA cleavage has occurred. This allows spontaneous strand fold back for hairpin formation. They were led to this conclusion by modeling exercises with all the known structures of nucleic acid hairpins docked into their structure; significant electrostatic repulsion or steric clashes were encountered for most attempts to fit the hairpins within the constrained space of the TelK dimer (20). Spontaneous strand foldback to form DNA hairpins has precedent in aberrant reactions of the closely related tyrosine recombinase family of enzymes (37, 38). Deletion of the analogous domain at the end of the C-terminal domain of ResT yields a cleavage defective resolvase.[3]

It is not currently known what role DNA bending may play in telomere resolution by ResT. However, the results in Fig. 3 with the LR and RL versions of the type 2 rTel indicate that substrate curvature affects telomere resolution. The L sequence possesses intrinsic curvature. Moving the L sequence from one side of the rTel to the other produces free reactions that have opposing biases in the ability to form the two hairpin telomeres, indicating a negative impact of this curvature

[3] Y. Tour and G. Chaconas, personal communication.

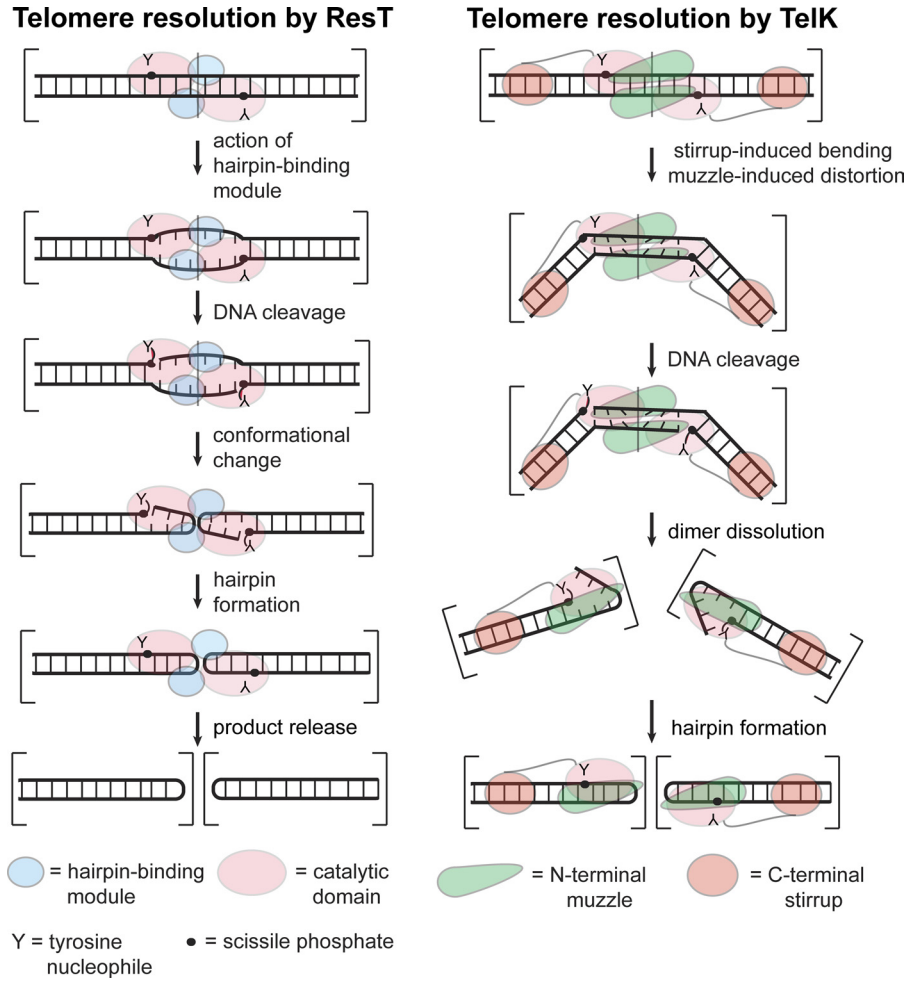

FIGURE 6. **A comparison of the current models of the telomere resolution reactions of ResT (*B. burgdorferi*) and TelK (*ϕ*KO2; *Klebsiella oxytoca*).** The reaction of ResT is pictured after the limiting step of substrate binding and dimerization. Once this complex is formed, the hairpin-binding module, found at the end of the N-terminal domain, engages the sequence between the scissile phosphates inducing a DNA distortion that can be mimicked by introduction of heteroduplex (25). This distortion seems to be required to allow the C-terminal catalytic domain to cleave and then rapidly hairpin the DNA followed by release of the hairpin telomeres (now pictured as encompassed by *two sets of brackets* instead of one set). The crucial feature of this model is that the energy of DNA distortion is used to license DNA cleavage and predispose the DNA strands for hairpin formation within the ResT-substrate complex. TelK binding and dimerization on its substrate is accompanied by significant substrate bending (73°) induced by the actions of the stirrup and muzzle domains. The stirrup, through interactions with distal sites in the substrate, induces the bend. The muzzle domain enforces a significant offset in this bend. This offset induces shear forces in the DNA between the cleavage sites buckling the basepairs between them. After DNA cleavage, this highly strained complex flies apart and the hairpins are formed by spontaneous strand fold back attacking the 3′-phosphotyrosine cleavage complexes closing the hairpins (20). The crucial feature of this model is that the energy of DNA bending/deformation is used for dimer dissolution, which in turn, allows spontaneous hairpin formation.

on hairpin formation. For the immobilized reactions, the rTel, in which the "L" sequence was bead proximal (the LR version), was more reactive than its RL counterpart. The rTels are immobilized via the bottom strand only (Fig. 3*A*), so one direction of intrinsic curvature relative to the bottom strand may be more conducive to reaction than the other. This possible role for DNA bending in telomere resolution by ResT requires further study. Substrates produced *in vivo* by replication through a hairpin telomere will always be perfectly dyad symmetric, in part, preventing the effects of intrinsic substrate DNA curvature from producing a serious bias in the formation of the two hairpin telomeres.

Our previous report that studied telomere resolution with substrates that blocked cleavage or hairpinning on one side of an rTel indicated that the chemical steps of telomere resolution could be uncoupled from each other (32). For the hairpin formation step of the reaction, this was particularly surprising as it implied that a hairpin telomere would be produced at the expense of also producing a deleterious ResT-capped double strand break. However, the use of immobilized substrates in this study allowed us to uncover a reaction mechanism for hairpin telomere formation that incorporates a requirement for both hairpin telomeres to be formed in the context of a ResT-DNA dimer complex prior to dissolution of this complex and release of the products. This mechanism of dual hairpin telomere formation preceding product release acts as a surveillance of the structural integrity of the telomeres and thereby protects the integrity genome as a whole.

Synapsis Independence of Telomere Resolution, Possible in Vivo Implications—We have demonstrated that the physical immobilization of replicated telomere junctions (rTels) does not prevent telomere resolution by ResT. This demonstrates that there is no requirement, intrinsic to the reaction mechanism of ResT, to synapse together rTels for telomere resolu-

tion. This argues against the reaction models II and III presented in Fig. 1. These synapsis-dependent models of telomere resolution were an attractive possibility because they afford a direct means of linking telomere resolution and chromosome segregation with cell division; synapsis of the rTel junctions at mid-cell to activate telomere resolution would allow a tight temporal/spatial link between these processes akin to that of the resolution of circular chromosome dimers by XerCD and FtsK at *dif* sites (39). The synapsis independence of telomere resolution *in vitro* and the fact that the origins of replication for several linear replicons in *B. burgdorferi* are thought to be asymmetrically disposed (40)[3] raises the possibility that DNA replication, in these cases, may give rise to Y-shaped replication intermediates in which one rTel has been resolved before the other telomere has been replicated. Such intermediates are a demonstrated feature of the replication of the hairpin telomere containing N15 linear prophage (17). Now, of course, *in vitro* reactions with short synthetic substrates and purified ResT fail to reproduce many important conditions in the cell that may influence telomere resolution. Substrate DNA supercoiling (41), presently unidentified accessory factors (15), possible resolvasome assemblies located at specific fixed cell loci, or coincident processes like DNA replication and transcription are all missing from our *in vitro* reactions. Although we have previously shown, *in vitro*, that ResT can form synapses of two rTels that form HJs, we do not know that such synapses are incapable of performing telomere resolution, just that they are not necessary. Therefore, a rigorous elimination of Model II will require a separate *in vivo* study of DNA replication and telomere resolution dynamics. Additionally, in such a study, it is possible different replicons may show different dynamics.

Acknowledgments—We thank Linda Chelico for critical reading of the manuscript. We also thank Yvonne Tourand and George Chaconas for communication of unpublished results.

REFERENCES

1. Schwan, T. G., Burgdorfer, W., and Rosa, P. A. (1999) in *Manual of Clinical Microbiology* (Murray, P. R., Baron, E. J., Pfaller, M. A., Tenover, F. C., and Yolken, R. H., eds.), 7th Ed., pp. 746–758, ASM Press, Washington, D.C.
2. Barbour, A. G. (2001) in *Emerging Infections 5* (Scheld, M. W., Craig, W. A., and Hughes, J. M., eds.), pp. 153–17, ASM Press, Washington, D.C.
3. Dworkin, M. S., Schwan, T. G., and Anderson, D. E., Jr. (2002) *Med. Clin. North Am.* **86,** 417–433
4. Stanek, G., and Strle, F. (2003) *Lancet* **362,** 1639–1647
5. Steere, A. C., Coburn, J., and Glickstein, L. (2004) *J. Clin. Invest.* **113,** 1093–1101
6. Barbour, A. G., and Garon, C. F. (1987) *Science* **237,** 409–411
7. Baril, C., Richaud, C., Baranton, G., and Saint Girons, I. S. (1989) *Res. Microbiol.* **140,** 507–516
8. Ferdows, M. S., and Barbour, A. G. (1989) *Proc. Natl. Acad. Sci. U.S.A.* **86,** 5969–5973
9. Casjens, S. (1999) *Curr. Opin. Microbiol.* **2,** 529–534
10. Picardeau, M., Lobry, J. R., and Hinnebusch, B. J. (1999) *Mol. Microbiol.* **32,** 437–445
11. Picardeau, M., Lobry, J. R., and Hinnebusch, B. J. (2000) *Genome Res.* **10,** 1594–1604
12. Nunes-Düby, S. E., Yu, D., and Landy, A. (1997) *J. Mol. Biol.* **272,** 493–508
13. Kobryn, K., and Chaconas, G. (2002) *Mol. Cell* **9,** 195–201
14. Byram, R., Stewart, P. E., and Rosa, P. (2004) *J. Bacteriol.* **186,** 3561–3569
15. Tourand, Y., Bankhead, T., Wilson, S. L., Putteet-Driver, A. D., Barbour, A. G., Byram, R., Rosa, P. A., and Chaconas, G. (2006) *J. Bacteriol.* **188,** 7378–7386
16. Deneke, J., Ziegelin, G., Lurz, R., and Lanka, E. (2000) *Proc. Natl. Acad. Sci. U.S.A.* **97,** 7721–7726
17. Ravin, N. V., Kuprianov, V. V., Gilcrease, E. B., and Casjens, S. R. (2003) *Nucleic Acids Res.* **31,** 6552–6560
18. Ravin, N. V. (2003) *FEMS Microbiol. Lett.* **221,** 1–6
19. Deneke, J., Burgin, A. B., Wilson, S. L., and Chaconas, G. (2004) *J. Biol. Chem.* **279,** 53699–53706
20. Aihara, H., Huang, W. M., and Ellenberger, T. (2007) *Mol. Cell* **27,** 901–913
21. Kobryn, K. (2007) in *Microbial Linear Plasmids* (Klassen, F. M. R., ed.) pp. 117–140, Springer-Verlag, Heidlberg, Germany
22. Moriarty, T. J., and Chaconas, G. (2009) *J. Biol. Chem.* **284,** 23293–23301
23. Huang, W. M., Joss, L., Hsieh, T., and Casjens, S. (2004) *J. Mol. Biol.* **337,** 77–92
24. Allingham, J. S., Wardle, S. J., and Haniford, D. B. (2001) *EMBO J.* **20,** 2931–2942
25. Bankhead, T., and Chaconas, G. (2004) *Proc. Natl. Acad. Sci.* **101,** 13768–13773
26. Grindley, N. D., Whiteson, K. L., and Rice, P. A. (2006) *Annu. Rev. Biochem.* **75,** 567–605
27. Kobryn, K., and Chaconas, G. (2005) *Mol. Cell* **17,** 783–791
28. Kobryn, K., Briffotaux, J., and Karpov, V. (2009) *Mol. Microbiol.* **71,** 1117–1130
29. Grindley, N. D. (1997) *Curr. Biol.* **7,** R608–612
30. Yu, K., and Lieber, M. R. (2000) *Mol. Cell. Biol.* **20,** 7914–7921
31. Tourand, Y., Deneke, J., Moriarty, T. J., and Chaconas, G. (2009) *J. Biol. Chem.* **284,** 7264–7272
32. Kobryn, K., Burgin, A. B., and Chaconas, G. (2005) *J. Biol. Chem.* **280,** 26788–26795
33. Thompson, J. F., and Landy, A. (1988) *Nucleic Acids Res.* **16,** 9687–9705
34. Tourand, Y., Lee, L., and Chaconas, G. (2007) *Mol. Microbiol.* **64,** 580–590
35. Haasnoot, C. A., de Bruin, S. H., Berendsen, R. G., Janssen, H. G., Binnendijk, T. J., Hilbers, C. W., van der Marel, G. A., and van Boom, J. H. (1983) *J. Biomol. Struct. Dyn.* **1,** 115–129
36. Davies, D. R., Goryshin, I. Y., Reznikoff, W. S., and Rayment, I. (2000) *Science* **289,** 77–85
37. Nash, H. A., and Robertson, C. A. (1989) *EMBO J.* **8,** 3523–3533
38. Zhu, X. D., Pan, G., Luetke, K., and Sadowski, P. D. (1995) *J. Biol. Chem.* **270,** 11646–11653
39. Barre, F. X., and Sherratt, D. (2002) in *Mobile DNA II* (Craig, N. L., Craigie, R., Gellert, M., and Lambowitz, A.M., eds.) pp. 149–161, ASM Press, Washington, D.C.
40. Picardeau, M., Le Dantec, C., and Vincent, V. (2000) *Microbiology* **146,** 305–313
41. Bankhead, T., Kobryn, K., and Chaconas, G. (2006) *Mol. Microbiol.* **62,** 895–905
42. Marshall, J. J., Gowers, D. M., and Halford, S. E. (2007) *J. Mol. Biol.* **367,** 419–431
43. Haniford, D. B. (2002) in *Mobile DNA II* (Craig, N. L., ed.) pp. 457–483, ASM Press, Washington, D.C.
44. Beaurepaire, C., and Chaconas, C. (2005) *Mol. Microbiol.* **57,** 132–142